Electronic Supplementary Material (ESI) for Soft Matter.

Supporting information

A novel supramolecular AIE π-gel for fluorescent detection and separation of metal ions from aqueous solution

Tai-Bao Wei*, Qin-Peng Zhang, Yan-Qing Fan, Peng-Peng Mao, Jiao Wang, Xiao-Wen Guan, You-Ming Zhang, Hong Yao and Qi Lin*

Key Laboratory of Polymer Materials of Gansu Province, Research Center of Gansu Military and Civilian Integration Advanced Structural Materials, College of Chemistry and Chemical Engineering, Northwest Normal University, Lanzhou 730070, China. E-mail: weitaibao@126.com; linqi2004@126.com.

Contents

Materials and methods

All the cations were purchased from Alfa Aesar Chemical, the anions were used from their tetrabutylammonium (TBA) salts and purchased from Sigmae Aldrich Chemical. They are stored in a vacuum desiccator. Fresh distilled water was used throughout the experiment. All other reagents and solvents were commercially available at analytical grade, which were used without further purification. ^{1}H NMR spectra were recorded on a Mercury-600 BB spectrometer at 600 MHz and a Mercury-400 BB spectrometer at 400 MHz. ^{13}C NMR spectra were recorded on a Mercury-600 BB spectrometer at 150 MHz and a Mercury-400 BB spectrometer at 101 MHz. The fluorescence spectra were recorded with a Shimadzu RF-5301 spectrofluorimeter. The FT-IR was performed on a Digilab FTS-3000 FT-IR spectrophotometer. Mass spectra were recorded on an esquire 6000 MS instrument equipped with an electrospray (ESI) ion source and version 3.4 of Bruker Daltonics Data Analysis as the data collection system. The X-ray diffraction analysis (XRD) was performed in a transmission mode with a Rigaku RINT2000 diffractometer equipped with graphite monochromated CuKa radiation (λ = 1.54073 Å).

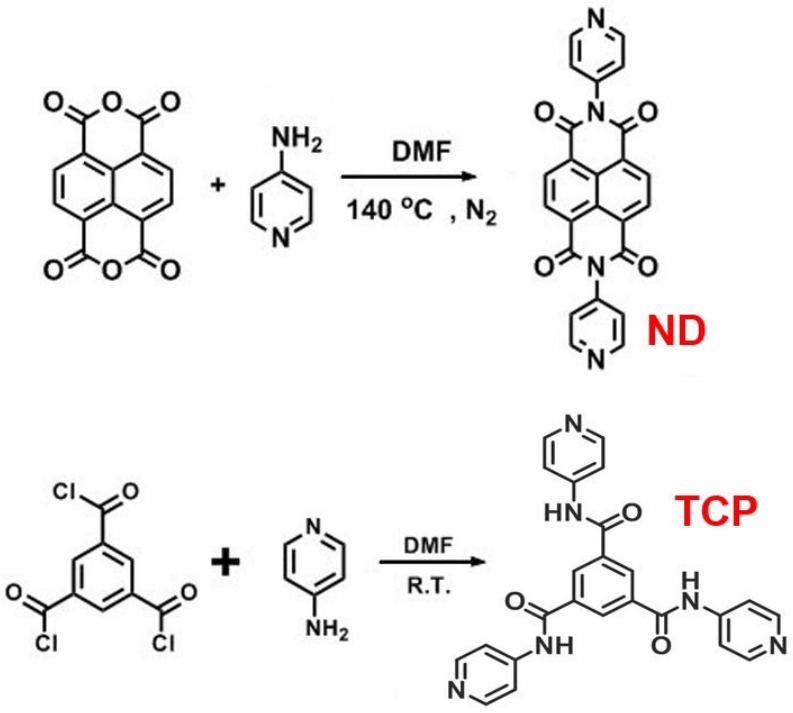

Scheme S1 Synthesis of **ND** and **TCP**.

Synthesis of ND

1,4,5,8-Naphthalene dianhydride (2.6 g, 10 mmol) and 4-aminopyridine (1.88 g, 20 mmol) was added into about 50 mL DMF in a reaction flask equipped with a stir bar and the reaction mixture was stirred for 72 h at 140 °C under N_2 atmosphere (Scheme S1). At the end of the reaction, the obtained black precipitate was filtered, washed three times with hot ethanol solution, and then recrystallized with DMSO solution and H_2O to give a pink powder product **ND** (3.381 g, yield: 80.5%, m. p. > 300 °C). ^{1}H NMR (DMSO-d_6, 600 MHz): δ 7.61-7.60 (t, 4 H), δ 8.75 (d, J = 5.1 Hz, 4 H), δ 8.83 and 8.82 (s, 4 H); ^{13}C NMR (DMSO-d_6, 150MHz): 162.90, 151.21, 144.11, 131.02, 127.45, 125.45; ESI-MS m/z: calcd [**ND**+H]$^+$ $[C_{24}H_{12}N_4O_4+H]^+$ = 421.0931; found: 421.0930.

Synthesis of TCP

The **TCP** was synthesized according to literature method. [S1] **TCP** was synthesized as follow: a solution of mixture of trimesoyl chloride (0.5278 g, 2.0 mmol) and triethylamine (1-2 d) was slowly added into the solution of 4-aminopyridine (0.6211 g, 6.6 mmol) in DMF (10 mL), the mixture was stirred at room temperature for 12 h, getting a white solid. The solid is vacuumed suction filtration and washed with cold ethanol solution (10 mL), finally the product solid was followed by drying in a vacuum oven at 40 °C for 24 h. (Yield: 90%. M.P.: 167 °C). ^{1}H NMR (400 MHz, DMSO-d_6, room temperature): δ 11.78 (s, 3 H), δ 8.99 (s, 3 H), δ 8.68 (m, 6 H), δ 8.25 (m, 6 H); ^{13}C NMR (DMSO-d_6, 150MHz): 165.68, 149.58, 135.07, 131.36, 114.75; ESI-MS m/: calcd [**TCP**+H]$^+$ for $[C_{24}H_{18}N_6O_3+H]^+$ = 439.1513; found: 439.1510.

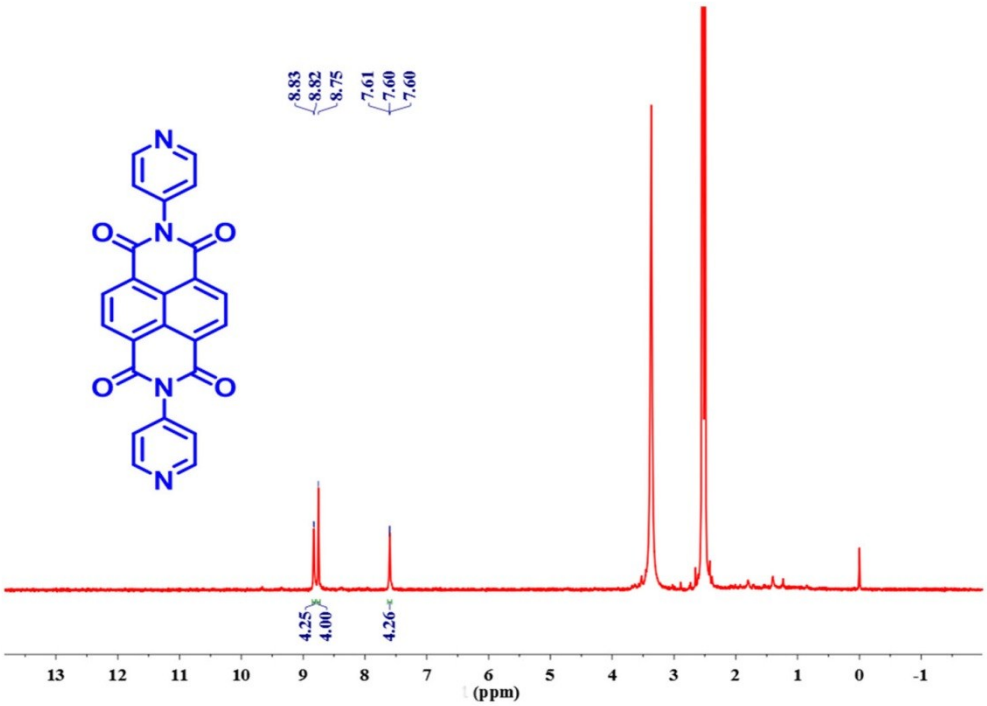

Fig. S1 The ^{1}H NMR spectra of **ND** in DMSO-d_6 (600 MHz, 298K).

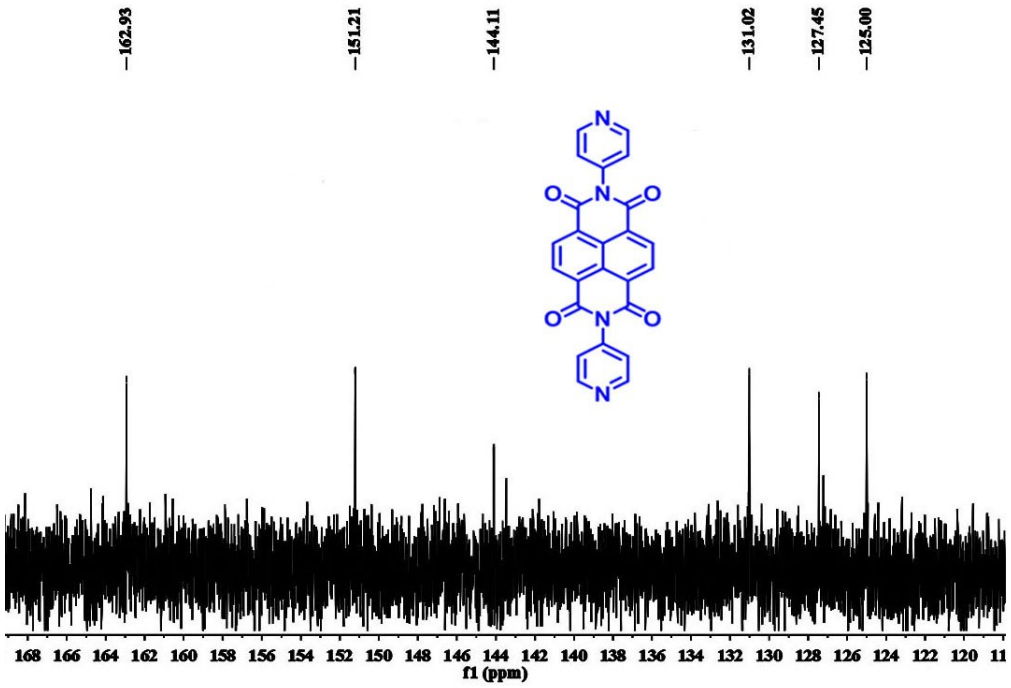

Fig. S2 The ^{13}C NMR spectra of **ND** in DMSO-d_6 (150 MHz, 298K).

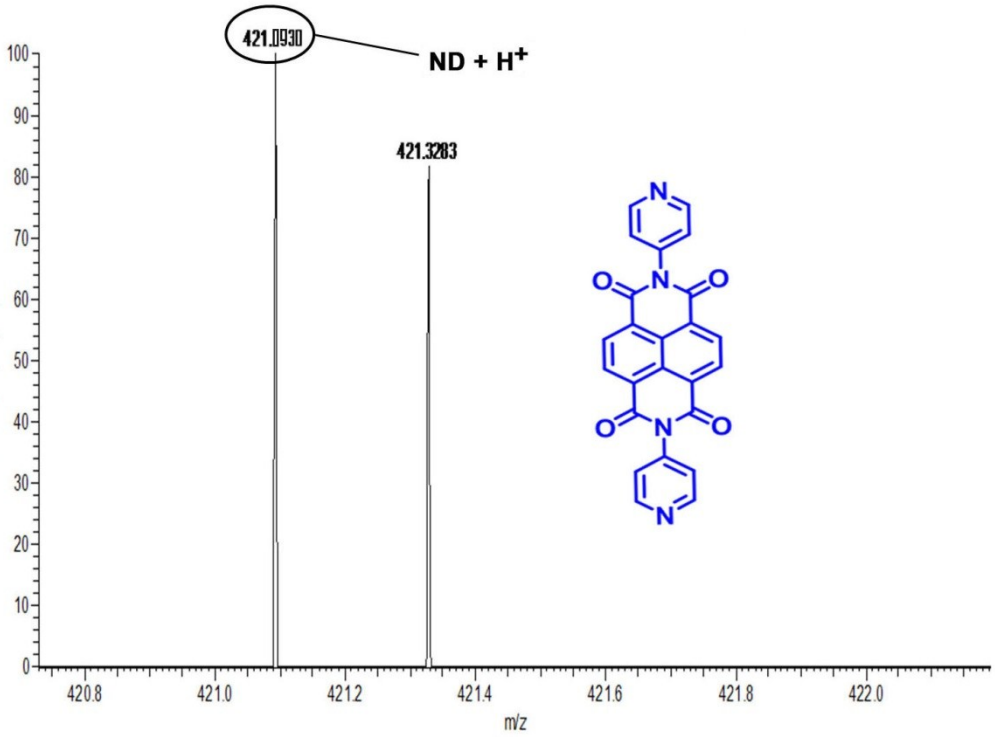

Fig. S3 ESI-MS spectra of compound **ND**.

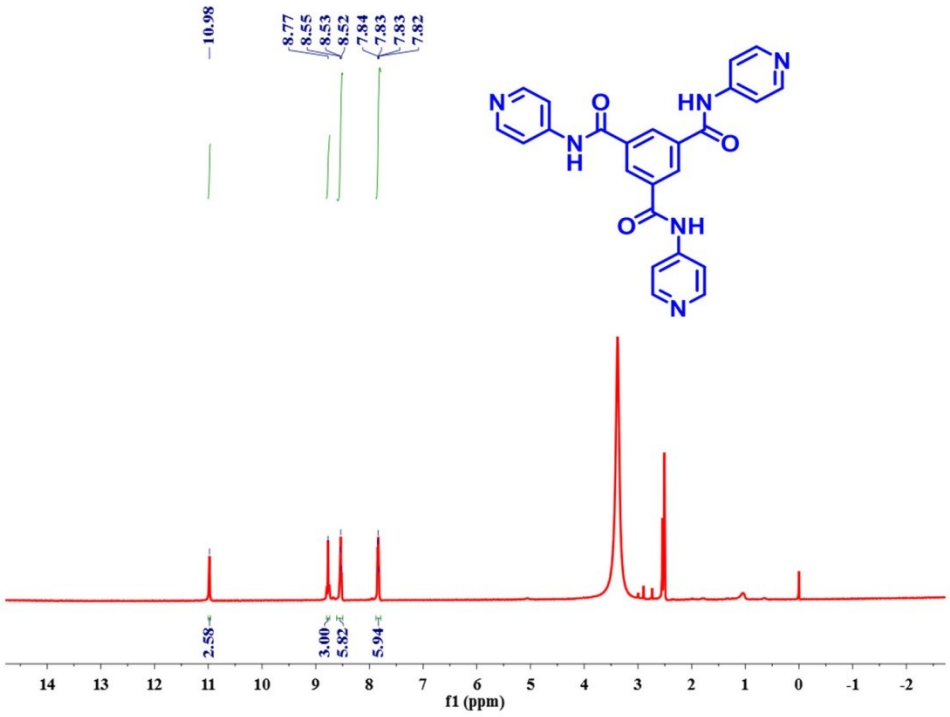

Fig. S4 ^{1}H NMR spectra of compound **TCP** in DMSO-d_6 (600 MHz, 298K).

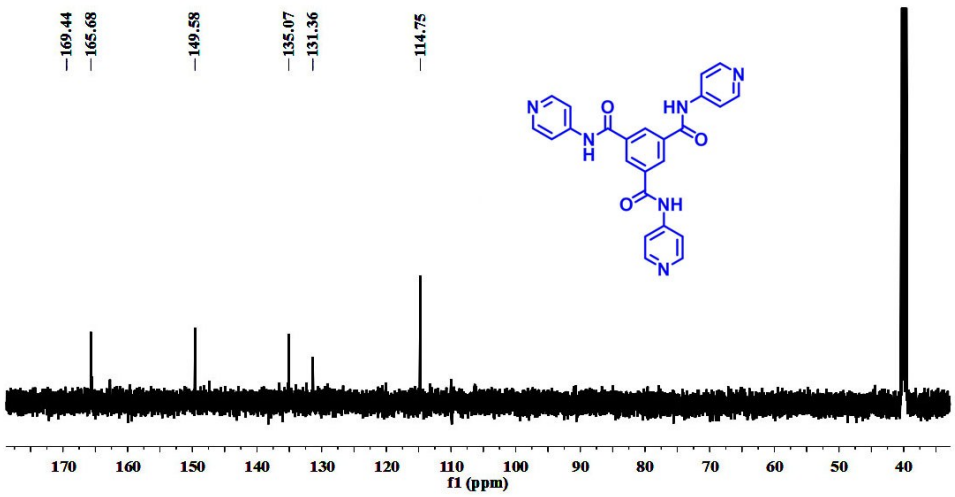

Fig. S5 The ^{13}C NMR spectra of **TCP** DMSO-d_6 (150 MHz, 298K).

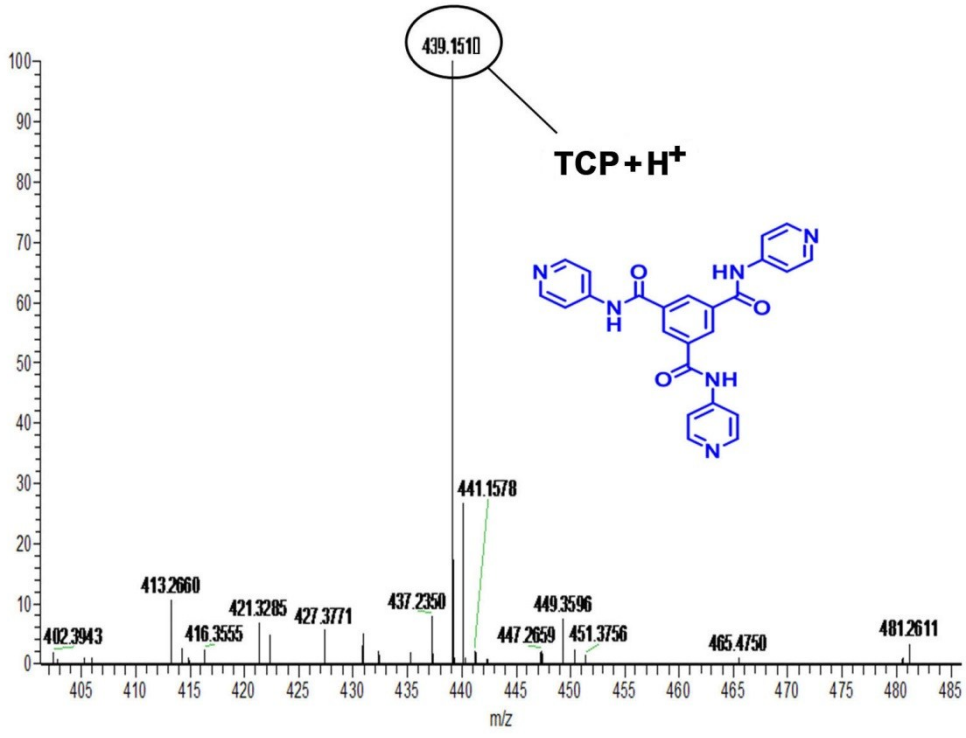

Fig. S6 ESI-MS spectra of **TCP**.

Table S1 Gelation behavior of the **ONT** in different solvents

Entry	Solvents	State[a]	CGC[b]	T^c_{gel} (°C, wt/v %)
1	Methanol	**P**	\	\
2	Ethanol	**P**	\	\
3	Isopropanol	**S**	\	\
4	n-Propanol	**S**	\	\
5	n-Butyl alcohol	**S**	\	\
6	n-Hexanol	**S**	\	\
7	Formic acid	**S**	\	\
8	Acetic acid	**P**	\	\
9	Propanoic acid	**P**	\	\
10	n-Butyric acid	**P**	\	\
11	Caproic acid	**P**	\	\
12	Ethyl acetate	**P**	\	\
13	Methylene	**P**	\	\
14	Chloride	**P**	\	\
15	Chloroform	**S**	**4**	**65**
16	DMF/H_2O	**P**	\	\
17	Acetonitrile	**G**	**3**	**76**
18	DMSO/H_2O	**P**	\	\
19	Glycerol	**P**	\	\

a: G, P and S denote gelation, precipitation and solution, respectively.

b: the critical gelation concentration (3%, wt%, 10 mg/mL=1%).

c: the gelation temperature (°C).

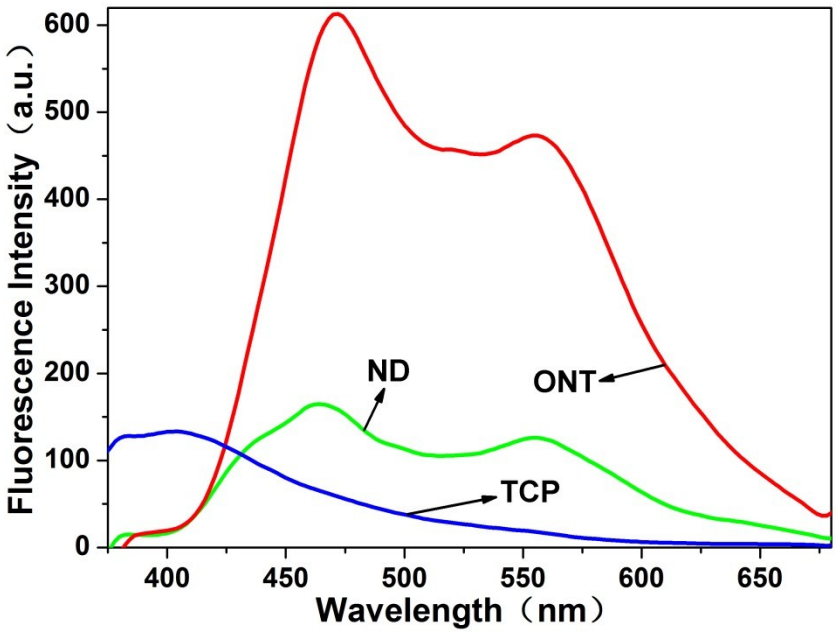

Fig. S7 Fluorescent spectra of the **ND**, **TCP** and the π-gel **ONT** in DMSO-H_2O (2:1, v/v) binary solution and λ_{ex} = 350 nm, respectively.

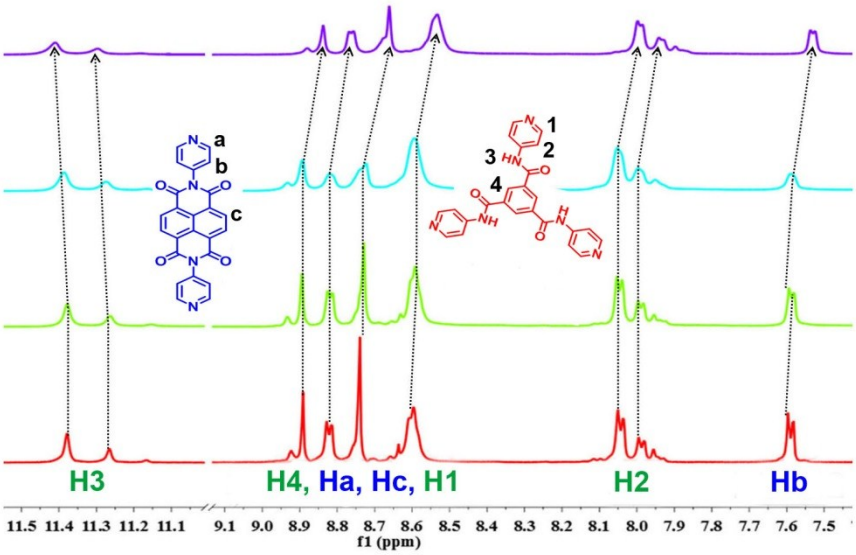

Fig. S8 Partial concentration-dependent ^{1}H NMR spectra (400 MHz, 298 K) of the **ONT**·at various concentrations: (a) 4.0 mM; (b) 8.0 mM; (c) 12.0 mM; (d)16.0 mM

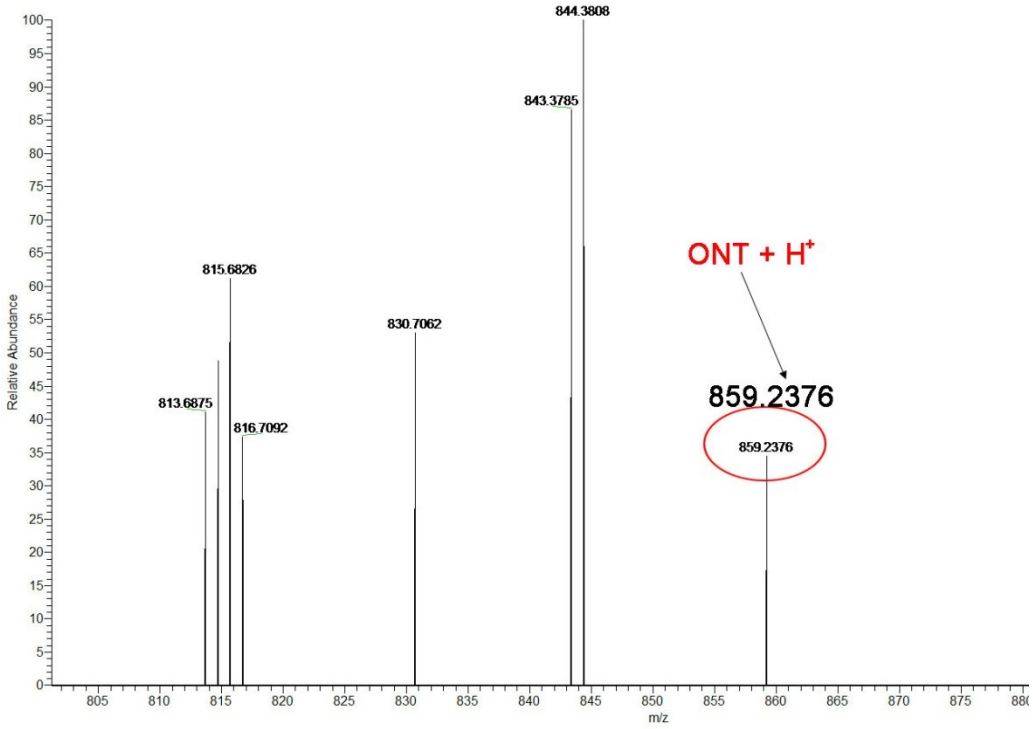

Fig. S9 ESI-MS spectra of the host-guest complex (**ONT**) formed between **ND** and **TCP**.

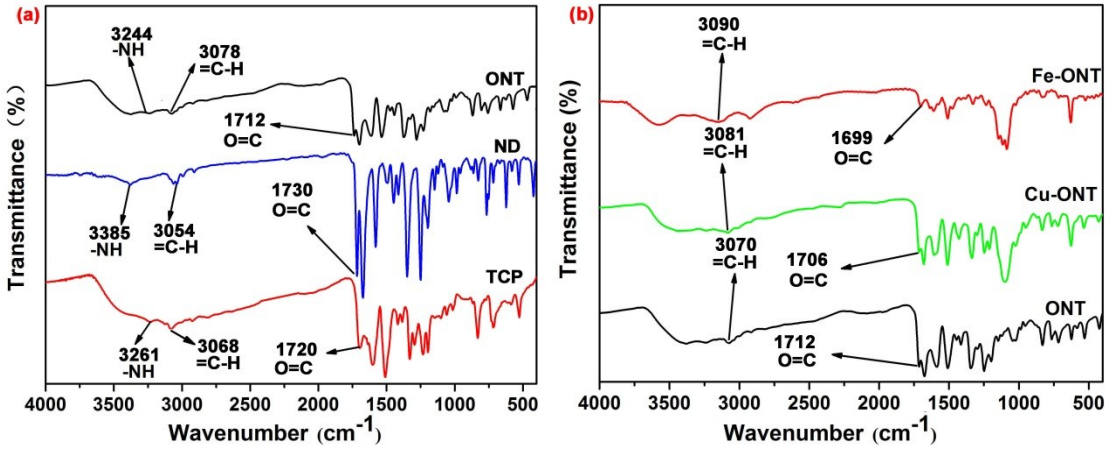

Fig. S10 FT-IR spectra of (a) Powder **ND**, **TCP** and xerogel **ONT**; (b) Xerogel **ONT**, **Fe-ONT** and xerogel **Cu-ONT**.

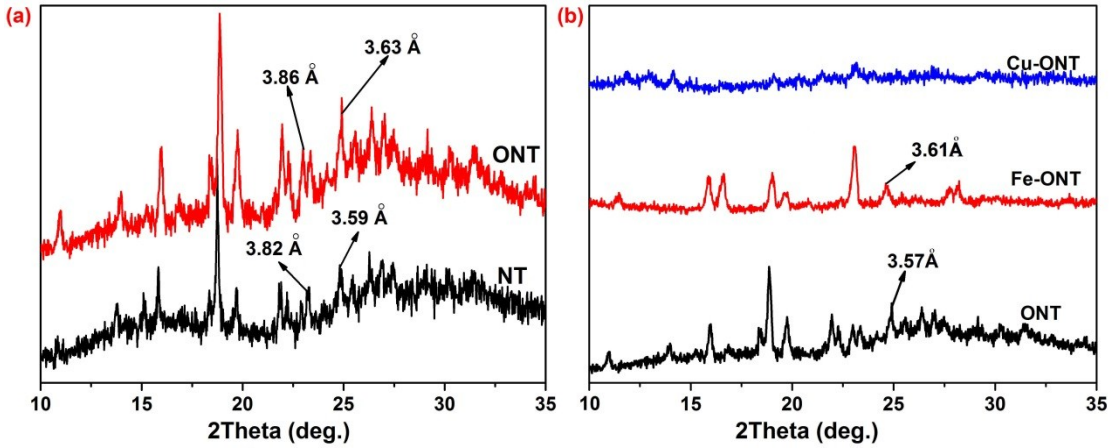

Fig. S11 XRD patterns of (a) Powder **NT** (the mixtures of **ND** and **TCP**) and xerogel **ONT**; (b) Xerogel **ONT**, xerogel **Fe-ONT** and xerogel **Cu-ONT**.

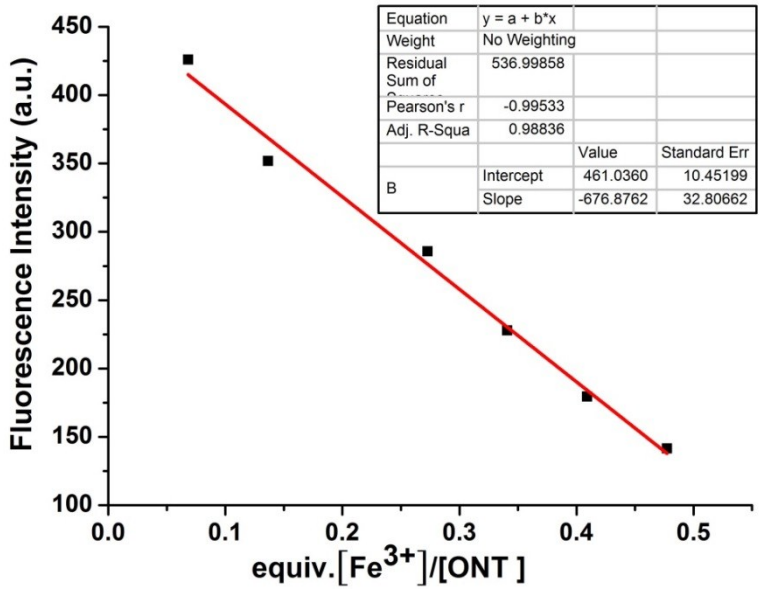

Fig. S12 The photograph of the linear range: the **ONT** for Fe^{3+}.

The result of the analysis as follows:

Linear Equation: Y = -616.8762 × X + 461.0360

R^2 = 0.98836 S = 6.17×10^8

$$\delta = \sqrt{\frac{\Sigma(Fi - F0)^2}{N - 1}} = 13.5735\ (N = 20)$$

LOD = K × δ/S = 6.60 × 10^{-8} M K=3

F_0 is fluorescence intensity of **ONT**, F_i is the average of fluorescence intensity F_0.

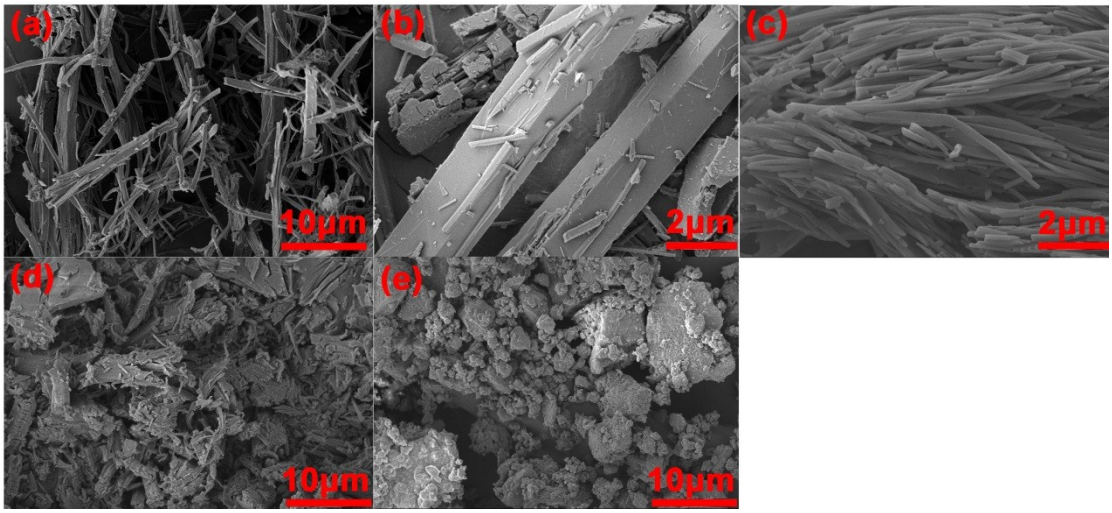

Fig. S13 SEM images of (a) Xerogel **ONT**; (b)Powder **ND**; (c) Powder **TCP**; (d) Xerogel **Fe-ONT**; (e) Xerogel **Cu-ONT**.

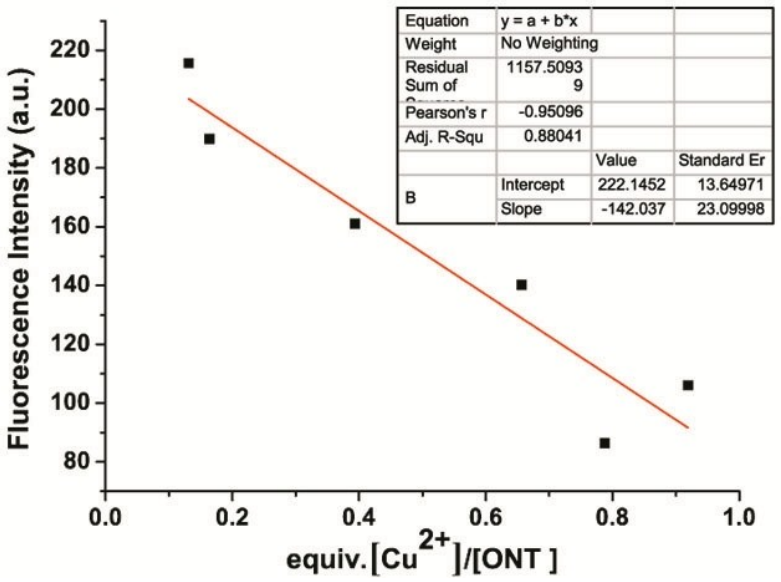

Fig. S14 The photograph of the linear range: the **ONT** for Cu^{2+}

The result of the analysis as follows:

Linear Equation: Y = -142.037 × X + 222.1452

R^2 = 0.88041 S = 1.42×10^{8}

$$\delta = \sqrt{\frac{\Sigma(Fi - F0)^2}{N-1}} = 8.2963\ (N = 20)$$

LOD = K × δ/S = 1.75×10^{-7} M

K = 3

F_0 is fluorescence intensity of **ONT**, F_i is the average of fluorescence intensity F_0.

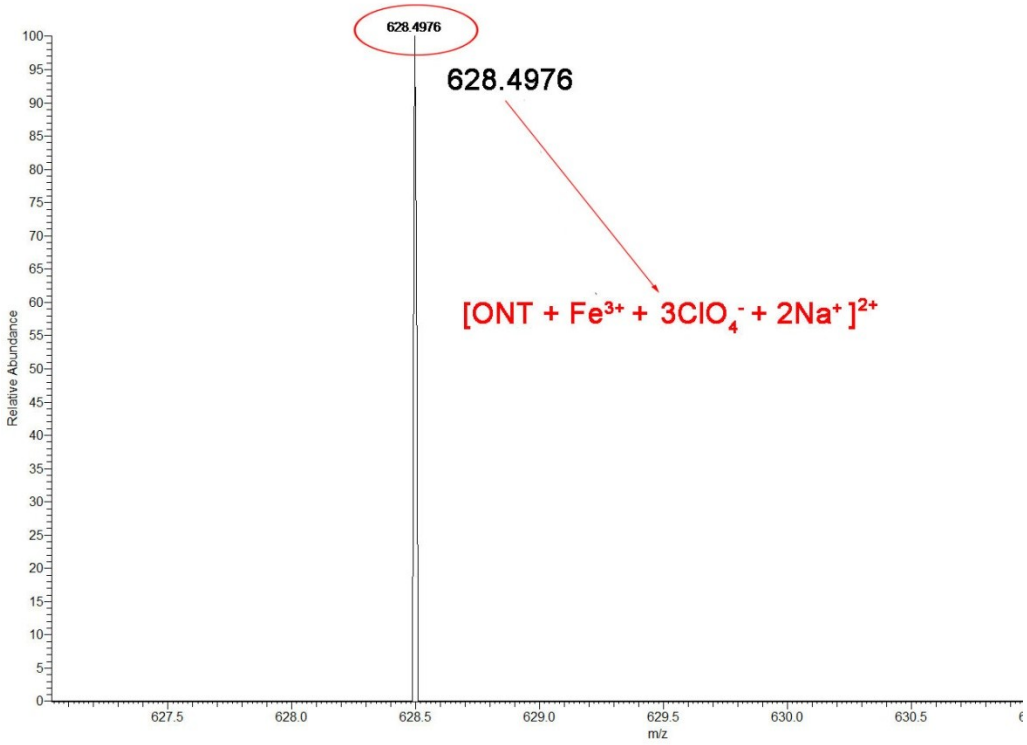

Fig. S15 The ESI-MS spectra of **Fe-ONT**.

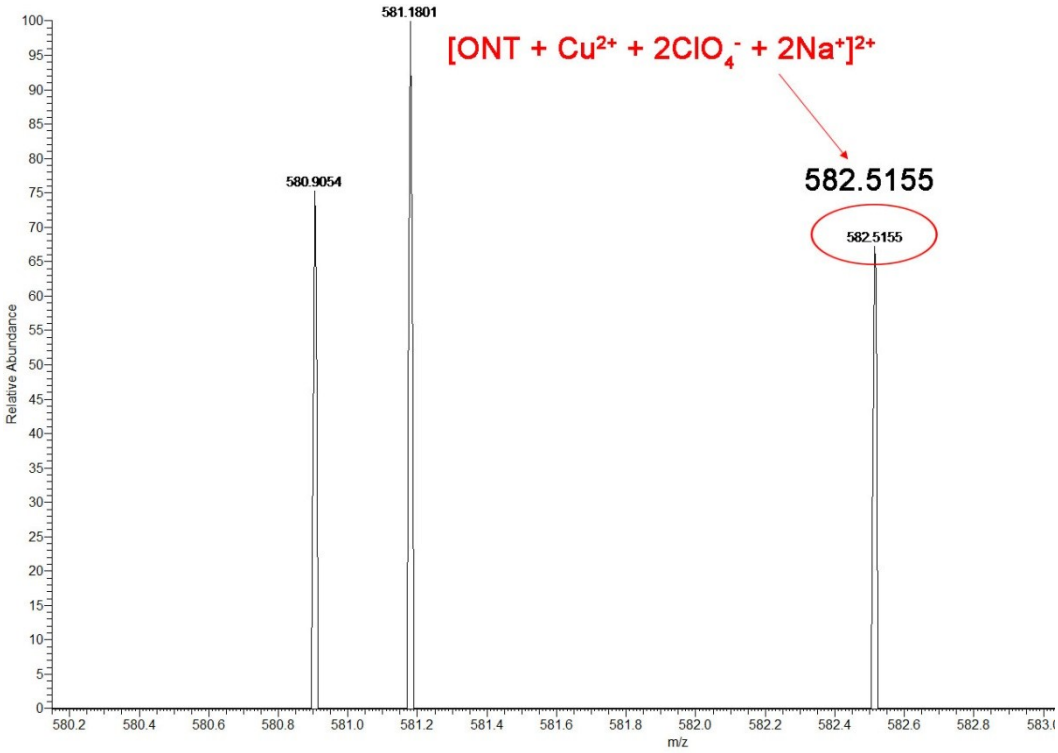

Fig. S16 The ESI-MS spectra of **Cu-ONT**.

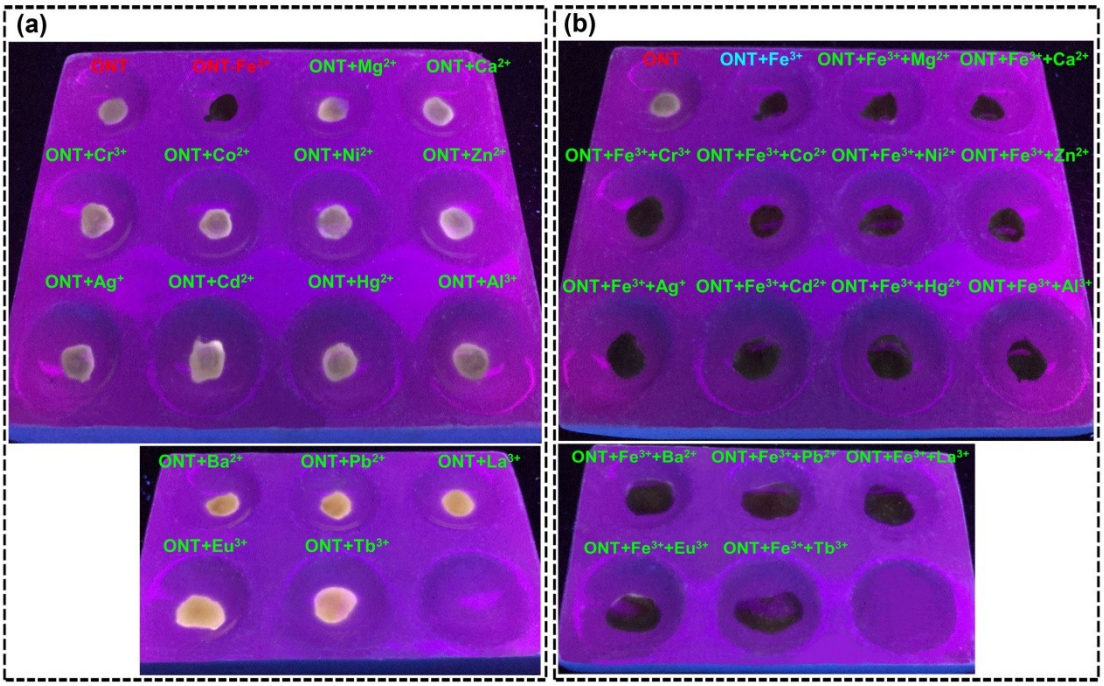

Fig. S17 The control experiment: the fluorescent responses of (a) the **ONT** and (b) the **Fe-ONT** to the presence of various cations (Fe^{3+}, Mg^{2+}, Ca^{2+}, Cr^{3+}, Co^{2+}, Ni^{2+}, Zn^{2+}, Ag^{+}, Cd^{2+}, Hg^{2+}, Al^{3+}, Ba^{2+}, Pb^{2+}, La^{3+}, Eu^{3+} and Tb^{3+}).

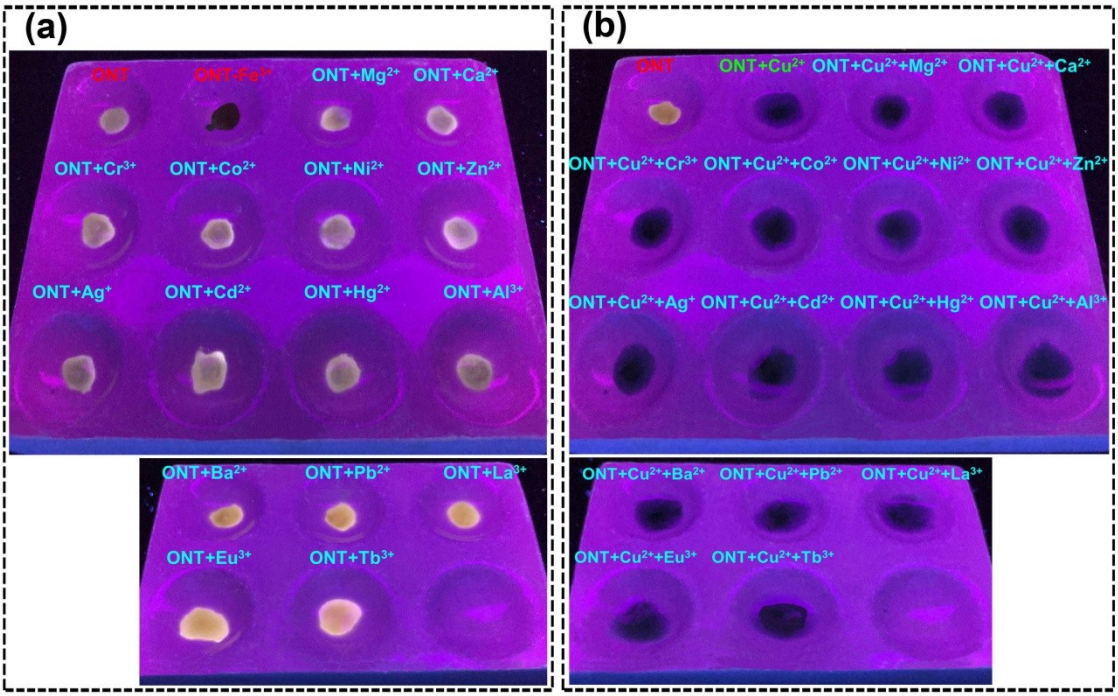

Fig. S18 The control experiment: the fluorescent responses of (a) the **ONT** and (b) the **Cu-ONT** to the presence of various cations (Cu^{2+}, Mg^{2+}, Ca^{2+}, Cr^{3+}, Co^{2+}, Ni^{2+}, Zn^{2+}, Ag^{+}, Cd^{2+}, Hg^{2+}, Al^{3+}, Ba^{2+}, Pb^{2+}, La^{3+}, Eu^{3+} and Tb^{3+}).

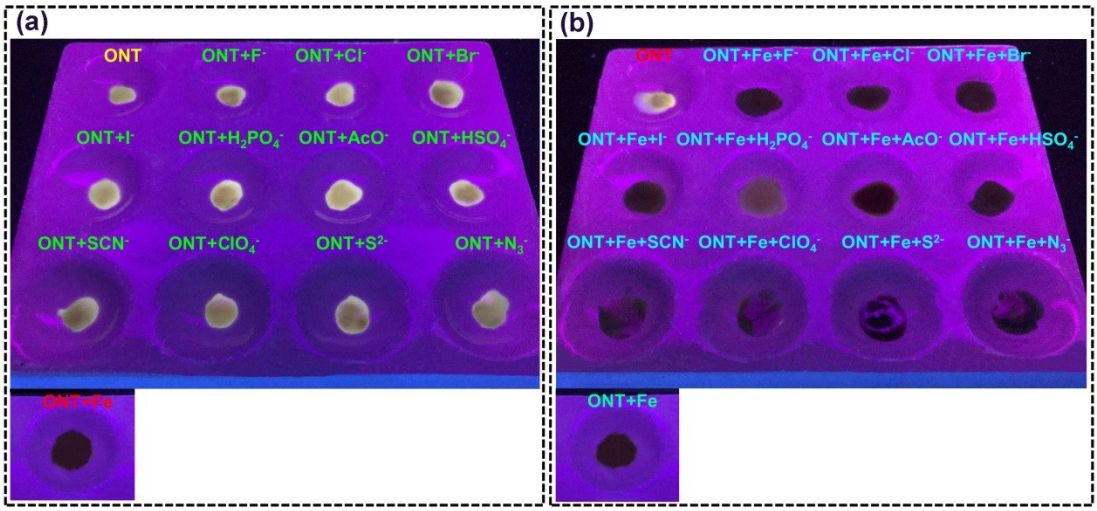

Fig. S19 The control experiment: the **Fe-ONT** treated by water solutions of various anions (F^-, Cl^-, Br^-, I^-, $H_2PO_4^-$, AcO^-, HSO_4^-, SCN^-, ClO_4^-, S^{2-} and N_3^-).

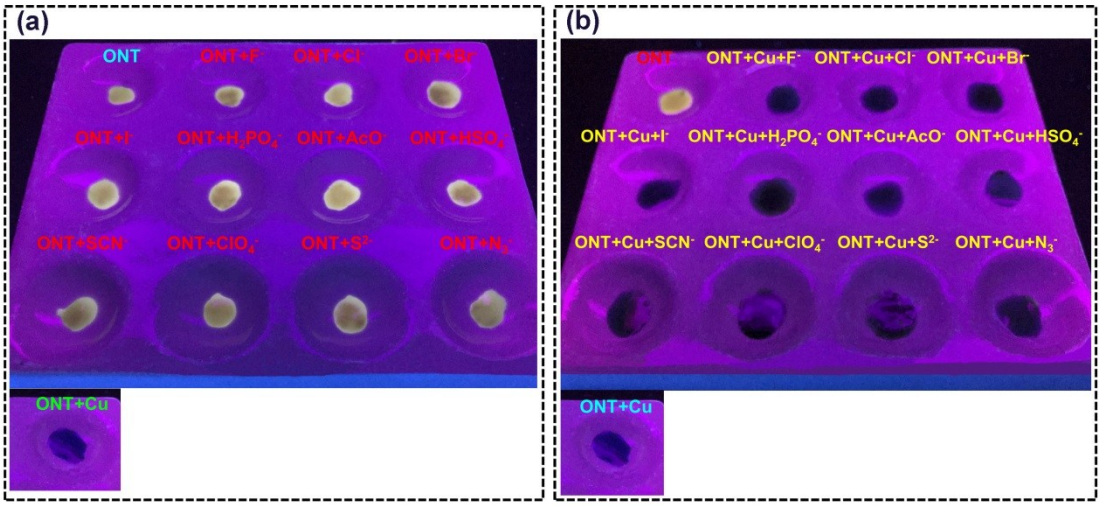

Fig. S20 The control experiment: the **Cu-ONT** treated by water solutions of various anions (F^-, Cl^-, Br^-, I^-, $H_2PO_4^-$, AcO^-, HSO_4^-, SCN^-, ClO_4^-, S^{2-} and N_3^-). cations (Fe^{3+}, Cu^{2+} and the mixtures of Fe^{3+} and Cu^{2+}).

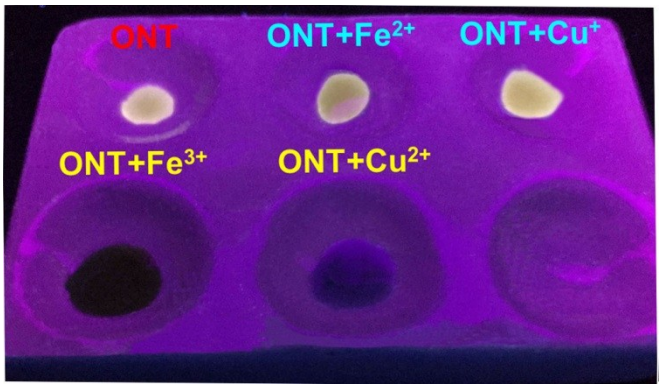

Fig. S21 The control experiment: the **ONT** treated by water solutions of various cations **(Fe^{2+}, Cu^{+}, Fe^{3+}** and **Cu^{2+})**.

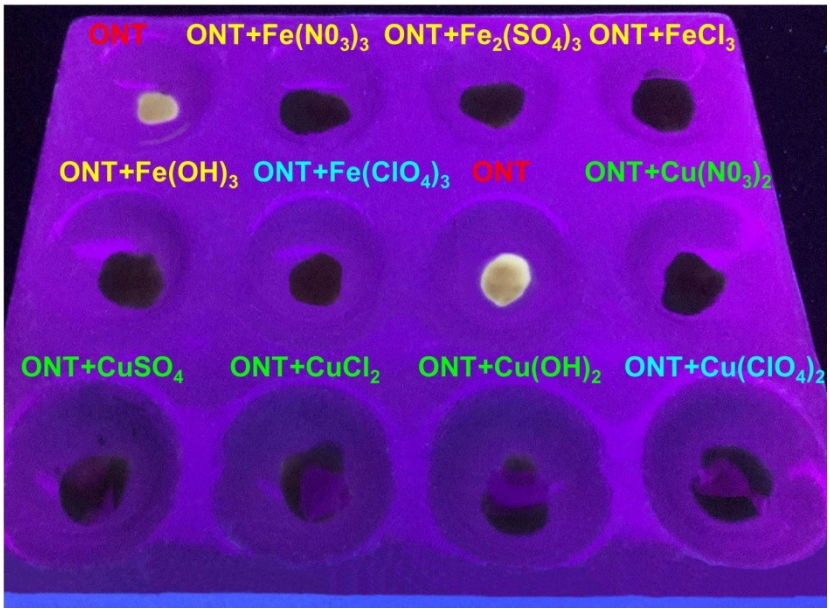

Fig. S22 The control experiment: the **ONT** treated by water solutions of various anions ($Fe(NO_3)_3$, $Fe_2(SO_4)_3$, $FeCl_3$, $Fe(OH)_3$, $Fe(ClO_4)_3$, $Cu(NO_3)_2$, $CuSO_4$, $CuCl_2$, $Cu(OH)_2$ and $Cu(ClO_4)_2$).

Table S2 Adsorption percentages of the **ONT** for Fe^{3+} and Cu^{2+}.

Entry	Ion	Initial concentration(M)	Residual concentration(M)	Absorbing rate(%)
1	Fe^{3+}	1×10^{-5}	0.65×10^{-6}	93.5%
2	Cu^{2+}	1×10^{-5}	0.83×10^{-6}	91.7%

Table S3 Comparison of the LODs and adsorption rates of different fluorescent Chemosensors for Fe^{3+}.

Refs	Fluorescent Chemosensors	LOD (μM)	Adsorption rate (%)
2	Azo and imine functionalized 2-naphthols	0.976	/
3	Bispillar[5]arene	0.156	/
4	Bis-naphthalimide functionalized pillar[5]arene	0.061	99.8%
5	Functionalized 1,4-benzenedicarboxylic acid	0.9	/
6	Graphene Quantum Dots	0.45	/
7	1-pyrene carboxyaldehyde derivative	0.26	/
8	Polyindole/cadmium sulphide nanocomposite	0.24	/
9	Aminoantipyrine	0.21	/
10	Pyrazoline derivative	1.40	/
11	2,5-diphenylfuran and 8-hydroxyquinoline	0.97	/
This work	Supramolecular AIE π-gel (**ONT**)	**0.066**	**93.5%**

Table S4 Comparison of the LODs and adsorption rates of different fluorescent Chemosensors for Cu^{2+}.

Refs	Fluorescent Chemosensors	LOD (μM)	Adsorption rate (%)
12	Phthalocyanine tetrasulfonic acid	0.55	/
13	Gold Nanoparticles	0.30	/
14	Fluorogenic cellulose membrane	0.73	/
15	O-phenylazo aniline	0.57	/
16	Ethylenediamine (EDA)	0.30	/
17	Pyridine coupled mono and bisbenzimidazoles	9.51	/
18	Pillar[5]arene derivative	0.1	96.96%
19	Coumarin derivative	0.37	/
20	4′-(4-Pyridinyl)-2,2′,6′,2″-terpyridine	3.98	/
21	Phenanthroimidazole derivative	0.87	
This work	Supramolecular AIE π-gel (**ONT**)	**0.175**	**91.70%**

References

(S1) Y. Q. Fan, J. Liu, Y. Y. Chen, X. W. Guan, J. Wang, H. Yao, Y. M. Zhang, T. B. Wei and Q. Lin, *J. Mater. Chem. C.*, 2018, **6**, 1333-13335.

(S2) A. Panja and K. Ghosh, *Mater. Chem. Front.,* 2018, **2**, 1866-1875.

(S3) T. B. Wei, J. F. Chen, X. B. Cheng, H. Li, B. B. Han, H. Yao, Y. M. Zhang and Q. Lin,

Polym. Chem., 2017, **8**, 2005-2009.

(S4) Y. M. Zhang, Y. F. Li, K. P. Zhong, W. J. Qu, H. Yao, T. B. Wei and Q. Lin, *New. J. Chem*., 2018, **42**, 16167-16173.

(S5) C. X. Yang, H. B. Ren, X. P. Yan, *Anal. Chem*., 2013, **85**, 7441-7446.

(S6) X. Zhu, Z. Zhang, Z. Xue, C. Huang, Y. Shan, C. Liu, X. Qin, W. Yang, X. Chen, T. Wang, *Anal. Chem*., 2017, **89**, 12054-12058.

(S7) S. D. Padghan, A. L. Puyad, R. S. Bhosale, S. V. Bhosale, S. V. Bhosale, *Photochem. Photobiol*. *Sci*., 2017, **16**, 1591-1595.

(S8) M. Faraz, A. Abbasi, F. K. Naqvi, N. Khare, R. Prasad, I. Barman, R. Pandey, *Sens. Actuators B*., 2018, **269**, 195-202.

(S9) Y. Zhou, H. Zhou, J. Zhang, L. Zhang, J. Niu, *Spectrochim. Acta. Part A*., 2012, **98**, 14-17.

(S10) S. Hu, S. Zhang, C. Gao, C. Xu, Q. Gao, *Spectrochim. Acta. Part A.,* 2013, **113**, 325-331.

(S11) S. Hu, G. Wu, C. Xu, J. Dong, Q. Gao,. *J. Photochem. Photobiol*. A., 2013, **270**, 37-42.

(S12) L. K. Kumawat, N. Mergu, A. K. Singh, V. K. Gupta, *Sens. Actuators. B*., 2015, **212***,* 389-394.

(S13) X. Xu, G. Duan, Y. Li, G. Liu, J. Wang, H. Zhang, Z. Dai, W. Cai, *ACS Appl. Mater. Interfaces*., 2014, **6***,* 65-71.

(S14) M. Li, Z. Liu, S. Wang, D. G. Calatayud, W. H. Zhu, T. D. James, L. Wang, B. Mao, H. N. Xiao, *Chem. Commu*n., 2018, **54***,* 184-187.

(S15) J. Jung, J. Jo, A. Dinescu, *Org. Process. Res. Dev*., 2017, **21***,* 1689-1693.

(S16) S. H. Yun, L. Xia, T. N. J. I. Edison, M. Pandurangan, D. H. Kim, S. H. Kim, Y. R. Lee, *Sens. Actuators. B*., 2017, **240***,* 988-995.

(S17) S. Panja, S. Bhattacharyab and K. Ghosh, *Mater. Chem. Front.,* 2018, **2***,* 385-395.

(S18) Q. Lin, Y. Q. Fan, P. P. Mao, L. Liu, J. Liu, Y. M. Zhang, H. Yao and T. B. Wei, *Chem. Eur. J*., 2018, **24**, 777-783.

(S19) X. J. Meng, S. L. Li, W. B. Ma, J. L. Wang, Z. Y. Hu, D. L. Cao, *Dyes. Pigments*., 2018, **154***,* 194-198.

(S20) J. F. Zhang, J. J. Wu, G. D. Tang, J. Y. Feng, F. M. Luo, B. Xu, C. Zhang, *Sens. Actuators. B*., 2018, **272**, 166-174.

(S21) S. M. Hwang, J. B. Chae and C. Kim, *Bull. Korean. Chem. Soc.* 2018, **39**, 925-930.